

Evolution of a FeV sigma phase ball-milled in a mixture of argon and air

B. F. O. Costa · G. Le Caër · B. Malaman

Published online: 28 October 2008
© Springer Science + Business Media B.V. 2008

Abstract A coarse-grained sigma phase $\text{Fe}_{48.1}\text{V}_{51.9}$ was ground in argon in a vibratory mill in the presence of a small but steady air supply. The oxygen content increases regularly at a rate of about 0.25 at.%/h. During the first 140 h of milling, the sigma phase transforms into a heterogeneous bcc alpha phase because of a preferential oxidation of the sole vanadium atoms into V_2O_3 . At that milling time, the average composition of the remaining bcc alloy is $\sim\text{Fe}_{80}\text{V}_{20}$. Mössbauer spectroscopy shows too the presence of an amorphous phase. For longer milling times, ternary Fe–V–O spinel phases do form.

Keywords Fe–V · Sigma phase · Ball-milling · Oxygen · Mössbauer spectroscopy

1 Introduction

According to the Fe–V equilibrium phase diagram, a disordered b.c.c. solid solution (α phase) is formed over an entire and broad composition range at high temperature which is interrupted at temperatures below 1,525 K by a tetragonal σ phase field

B. F. O. Costa (✉)
CEMDRX, Department of Physics,
University of Coimbra, 3004-516 Coimbra, Portugal
e-mail: benilde@ci.uc.pt

G. Le Caër
Institut de Physique de Rennes, UMR UR1-CNRS 6251,
Université de Rennes I, Campus de Beaulieu, Bat. 11A,
35042 Rennes Cedex, France

B. Malaman
LCSM UMR CNRS 7555, Université Henri Poincaré-Nancy I,
BP239, 54506 Vandoeuvre-les-Nancy Cedex, France

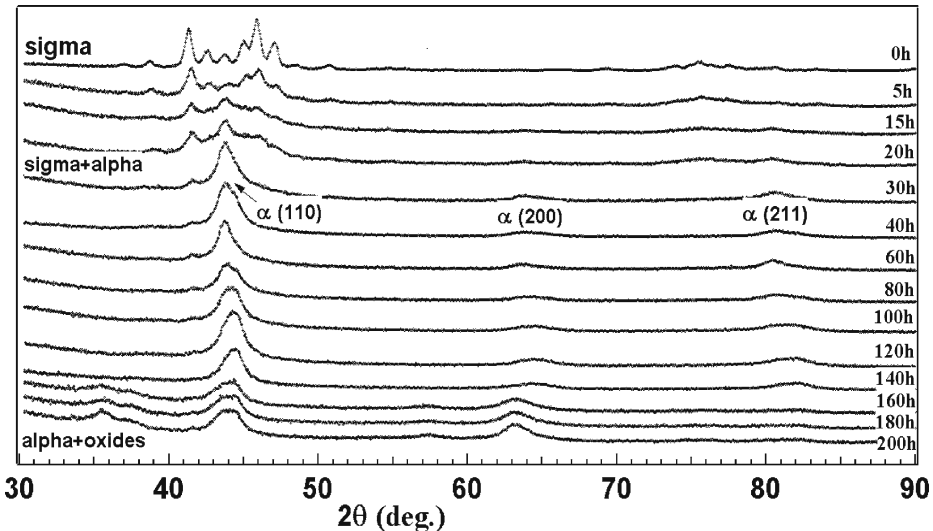


Fig. 1 X-ray diffraction patterns of a σ -FeV powder milled for the indicated periods

for near equiatomic compositions [1, 2]. Owing to the slow kinetics of the $\alpha!\sigma$ transformation, the formation of the σ -phase can be bypassed kinetically and a disordered bcc phase, A2, can be obtained at low temperatures by rapid cooling.

Mechanical alloying [3–5] of mixtures of elemental powders of Fe and V and grinding of as-prepared Fe–V alloys were investigated by various authors [6–14]. Milling of blends of elemental powders in a conventional ball mill, in argon atmosphere, resulted in the formation of a bcc phase even in concentrated alloys for which the stable phase at 300 K is the σ phase. Amorphous FeV alloys or admixtures of bcc and amorphous phases were instead reported to form by mechanical alloying of equiatomic FeV blends in nitrogen. Although clean co-evaporated Fe–V thin films are amorphous and paramagnetic down to 4 K when the V content ranges between 0.45 and 0.55 [15], the formation of amorphous phases by milling is clearly favored by the presence of oxygen. This might explain why different phases are reported to occur according to the milling conditions. Ziller [16] investigated the mechanically alloying in a planetary high-energy ball-mill of $\text{Fe}_{0.50}\text{V}_{0.50}$ and $\text{Fe}_{0.35}\text{V}_{0.65}$ mixtures of elemental Fe and V powders in argon and in conditions described too in [14]. When the V powders were stored in air without care, the milled powders were found to be predominantly amorphous. The neutron patterns, characteristics of amorphous phases [16], show broad haloes whose amplitudes and positions are reminiscent of the pattern of the σ phase (Fig. 1) with its three main bunches of peaks. For prolonged milling, the amorphous phase was observed to crystallize and an oxide was observed to form. It was tentatively attributed to “VO”, possibly off-stoichiometric. The oxygen contents of such ground powders (~3 wt.%) were found to be significantly higher than those of ground alloys containing a small fraction of amorphous phase. The σ -FeV phase transforms into a α phase when ground in vacuum and in argon [3, 11].

To better understand the role of residual gases on the stability of a near-equiatomic σ -FeV under ball-milling, we ground the latter phase firstly in argon in the presence of a steady air supply and secondly in vacuum (to be published), using X-ray diffraction and ^{57}Fe Mössbauer spectroscopy as the main characterization techniques of the structural evolution. The steady increase of the oxygen content is further a way to follow the effect of a preferential oxidation of one of the constitutive element of a ground binary compound which competes with the transformations which occur usually in the absence of air. The present paper reports then on the influence of oxygen on the phase changes with milling time t_m , essentially up to $t_m = 140$ h.

2 Experimental

The starting $\text{Fe}_{48.1}\text{V}_{51.9}$ at.% alloy was prepared by melting together, in argon, appropriate amounts of Fe (>99.9% purity) and V (99.7% purity) in an induction furnace. The composition is close to that studied by Bakker et al. [3]. The sigma phase was formed by annealing the as-cast bcc alloy in vacuum at 1,000°C for 100 h. The brittle sigma phase was finally powdered, with a pestle in an agate mortar, into particles of about 90 μm . A mass of about 5 g of σ -FeV was then ball-milled in accumulated milling times in a Fritsch P0 mill at its maximum amplitude of vibration (3 in scale). The mill consists of a hardened steel vial with a hardened steel ball whose diameter is 5 cm and whose mass is 500 g. The vial cover was home made to permit an easy filling of the vial with argon. Air penetrated steadily in the vial through a small hole of a diameter of $90 \pm 10 \mu\text{m}$.

X-ray diffraction (XRD) was carried out at room-temperature (RT) using Cu K_α radiation ($\lambda = 0.15406$ nm). The mean crystallite size and the mean microstrain were obtained from the widths of the XRD peaks using the Williamson–Hall method [17].

^{57}Fe Mössbauer spectra were recorded at RT in a transmission geometry using a standard constant acceleration spectrometer. A ^{57}Co source in Rh matrix with a strength of ≈ 25 mCi was used. The spectra were analysed by a constrained Hesse–Rübartsch method [18], which yields a hyperfine magnetic field distribution (HMF_D), P(B), where P(B)dB represents the fraction of Fe atoms whose field is between B and B+dB. The average of any parameter Y(B) will be denoted as $\langle Y \rangle$. Lorentzian line-shapes were employed in this procedure. The ^{57}Fe isomer shifts are given with respect to α -Fe at RT.

3 Results and discussion

Compositions of $\text{Fe}_{48.1}\text{V}_{51.9}$, $\text{Fe}_{49.5}\text{V}_{50.5}$, $\text{Fe}_{51.2}\text{V}_{48.8}$ and $\text{Fe}_{52.3}\text{V}_{47.7}$ at.%, expressed here for the sole metal elements, were determined by microprobe analysis for the starting alloy and for alloys milled for 60, 140 and 200 h, respectively. The sample milled for 140 h is denoted bm140 hereafter. The oxygen contents of these milled samples are 16.8, 35.4 and 50.5 at.%, respectively, while the nitrogen contents are 0.62, 0.51 and 0.22 at.%, respectively. The oxygen content increases regularly at a rate of about 0.25 at.%/h. The nitrogen contents remain small when compared with the oxygen contents. No trace of argon was detected in the milled samples.

Fig. 2 RT ^{57}Fe Mössbauer spectra of a σ -FeV powder milled for different periods and the associated HFMD's: **a** starting sigma phase; **b** 15 h; **c** 30 h; **d** 60 h; **e** 80 h; **f** 100 h; **g** 120 h; **h** 140 h

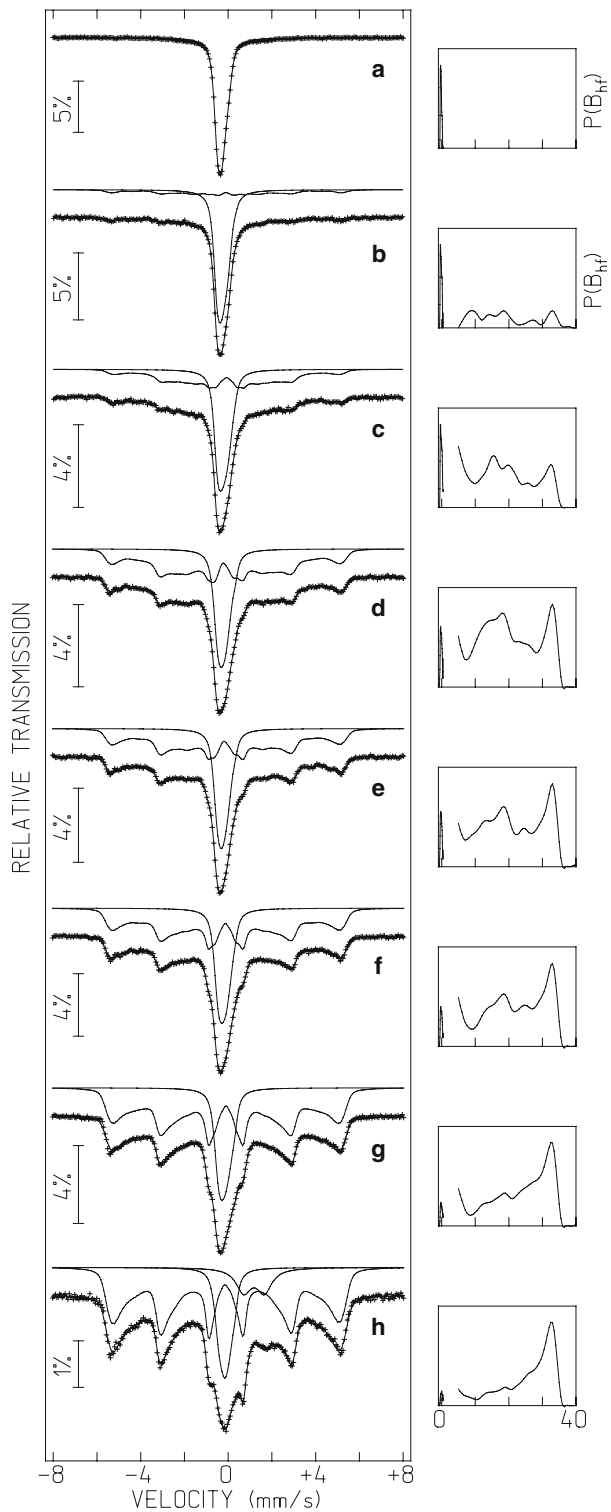


Fig. 3 Thinned RT ^{57}Fe Mössbauer spectra [20] of a $\sigma\text{-FeV}$ powder milled for 140 h in a mixture of argon and air (solid line-empty circles) and of a p- $\text{Fe}_{50}\text{V}_{50}$ elemental powder mixture milled for 4 h in argon in a Fritsch planetary ball-mill [16] (solid line-crosses)

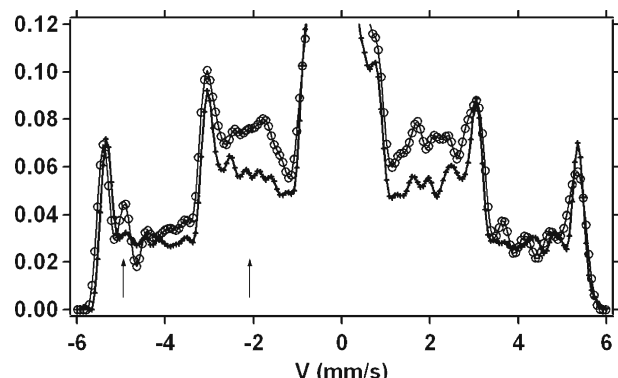


Figure 1 shows the X-ray diffraction patterns of the starting $\sigma\text{-FeV}$ milled for different periods. After 5 h of milling, the X-ray diffraction peaks broaden as a consequence of a refinement of crystallite sizes and of strain.

After 15 h of milling, new peaks ascribed to the bcc alpha phase appear. For milling up to 140 h (Fig. 1), the samples remain essentially bcc with broadened peaks. For prolonged milling, from 160 to 200 h, new diffraction lines appear, they are due to bcc Fe–V, fcc Fe–V alloys and to ternary oxide phases. The oxide peaks are attributed to V_2O_3 with a corundum type structure and to a defective $\text{Fe}_{1-y}\text{V}_{2(1-y)}\text{W}_{3y}\text{O}_4$ spinel with Fe^{2+} and V^{5+} cations and with vacancies on both sites.

The average grain size of the bcc phase decreases from ~ 9 nm after 20 h of milling to ~ 5 nm after 100 h and remains constant for longer milling times. The microstrain has a typical value of $\sim 2.5\%$. The RT lattice parameters of bcc Fe, of disordered bcc FeV and of bcc V are reported to be $a(\text{bcc}) = 0.28665, 0.2906$ and 0.30271 nm respectively [1, 2, 19]. The lattice parameter $a(\text{bcc})$ decreases regularly up to $t_m = 140$ h down to $0.2884(4)$ nm while it increases for milling times longer than 160 h. From the concentration dependence of the lattice parameter of the disordered bcc phase [19], the bcc alloy milled for $t_m = 140$ h is concluded to be $\text{Fe}_{82 \pm 4}\text{V}_{18 \pm 4}$.

Figure 2 shows RT ^{57}Fe Mössbauer spectra and hyperfine magnetic field distributions for samples milled up to 140 h. The starting sigma phase is paramagnetic at RT with an average isomer shift $\langle IS \rangle = -0.20$ mm/s. Between ~ 30 and 120 h of milling, a magnetic component shows a narrow peak at a field which is identical with or close to the field of $\alpha\text{-Fe}$ at RT and a broad band from ~ 10 to ~ 30 T (Fig. 2). Figure 3 compares the bm140 spectrum with that of an elemental powder mixture $\text{Fe}_{50}\text{V}_{50}$, denoted p- $\text{Fe}_{50}\text{V}_{50}$, milled for 4 h in a Fritsch P7 planetary ball-mill [13, 14, 16]. For an easier comparison, both are ‘thinned’ with the method of deconvolution of a Lorentzian line (full-width at half-maximum $\Gamma = 0.22$ mm/s) described in Section 7.2 of [20] and plotted upwards for that reason. Rather flat and essentially featureless broad bands are observed between the sharp external, intermediate and internal ‘ $\alpha\text{-Fe}$ ’ peaks of the p- $\text{Fe}_{50}\text{V}_{50}$ spectrum. Arrows (Fig. 3) are plotted to draw the attention to the main differences between the two sharpened spectra. The left arrow emphasizes the fact that the peak due to Fe atoms which have a V atom as a nearest-neighbour is much clearer for the bm140 spectrum than for the p- $\text{Fe}_{50}\text{V}_{50}$ spectrum. A rather well-defined Fe-rich Fe–V solid solution is then formed in the bm140 sample. Simultaneously, the right arrow emphasizes the existence of

components with rather low hyperfine fields in the bm140 spectrum that are not seen in the p-Fe₅₀V₅₀ spectrum (the small doublet discussed below does not contribute to the absorption in that velocity range). They are due to concentrated FeV bcc alloys. The mean V content in bm140 is calculated from the average hyperfine field $\langle B(140 \text{ h}) \rangle = 26.2 \text{ T}$ to be 21 ± 2 from the literature values [21–23]. It is in good agreement with that, 18 ± 4 , deduced from X-ray diffraction patterns. Knowing the alloy compositions from chemical analyses and assuming the formation of V₂O₃ allows us to calculate the average content as a function of milling time. The average V content of the bm140 sample is found to be 20 ± 2 , a value consistent with the two previous values. Details shall be given elsewhere.

The central parts of the spectra (Fig. 2), which are due to non-magnetic phases at RT, evolve with milling time. The mean isomer shift $\langle IS \rangle_c$ changes with milling time, with a plateau at $\langle IS \rangle_c = -0.18 \text{ mm/s}$ from 15 h of milling to 80 h of milling. Then, $\langle IS \rangle_c$ increases up to -0.039 mm/s for 140 h of milling while the associated area percentage is 18%. The central component at $t_m = 140 \text{ h}$ is no longer due to the sigma phase but to a non-magnetic amorphous phase whose shift agrees with that of co-evaporated near-equiautomatic Fe–V amorphous alloys [14]. In addition, the bm140 spectrum (Fig. 2) shows the emergence a broad doublet due to Fe²⁺, with a quadrupole splitting QS = 0.96 mm/s, an isomer shift IS = 1.30 mm/s and a full width at half maximum $\Gamma = 0.83 \text{ mm/s}$.

4 Conclusion

The evolution of the FeV sigma phase ball-milled in the presence of air may be sketched as follows. Vanadium atoms react preferentially with oxygen during milling to form a nanostructured vanadium oxide, V₂O₃. Its nanocrystallinity explains why it is not observed on diffraction patterns. The bcc alloy around these oxide particles (or oxide films at grain boundaries for instance) is locally depleted in vanadium. Therefore, the bcc phase becomes globally heterogeneous as reflected by the observed HMFDS's. Notable is the fact that Fe atoms begin to form ternary oxides, after about 140 h of milling. These results can be understood in the light of a mechanism which is discussed elsewhere (in preparation), based on oxygen-vacancy pairs, put forward recently to account for the ultrahigh stability of oxide nanoclusters in ODS Fe-based alloys processed by ball-milling [24].

Part of the concentrated bcc Fe-V alloy transforms into an amorphous phase as observed when milling the sigma phase in the absence of air. These preferential oxidation reactions, which compete with the usual phase transformations which take place in the absence of oxygen, occur at moderate temperatures in the mild conditions of milling of the vibratory mill used in the present work.

Acknowledgements The financial support of the bilateral Portuguese-French program PESSOA (grant no 14617RE) is gratefully acknowledged.

References

1. Kubaschewski, O.: Iron-binary phase diagrams, pp. 160–164. Springer, Berlin (1982)
2. Villars, P., Calvert, L.D.: Pearson's handbook of crystallographic data for intermetallic phases. In: American Physical Society for Metals, pp. 2246. Metals Park, OH (1991)

3. Bakker, H., Zhou, G.F., Yang, H.: Mechanically driven disorder and phase transformations in alloys. *Prog. Mater. Sci.* **39**, 159–241 (1995)
4. Yang, H., Bakker, H.: Formation of amorphous and metastable phases from the sigma phase by ball milling. *Mater. Sci. Eng., A.* **181/182**, 1207–1211 (1994)
5. Suryanaryana, C.: Mechanical alloying and milling. *Prog. Mater. Sci.* **46**, 1–184 (2001)
6. Fultz, B., Le Caer, G., Matteazzi, P.: Mechanical alloying of Fe and V powders: intermixing and amorphous phase formation. *J. Mater. Res.* **4**(6), 1450–1455 (1989)
7. Lanote, L., Matteazzi, P.: Influence of grinding on magnetic properties of Fe–V and Fe powders. *J. Magn. Magn. Mater.* **88**, 58–62 (1990)
8. Fukunaga, T., Mori, M., Misawa, M., Mizutani, U.: Structural observation of metastable phases prepared by MA in V–M(=Fe, Cu) systems. *Mat. Sci. Forum* **88–90**, 663–670 (1992)
9. Rawers, J., Doan, R.C., Slavens, G., Govier, D., Siple, J.: Effects of mechanical alloying of iron alloys in a gaseous nitrogen atmosphere. *J. Mater. Synth. Process.* **1**, 75–84, (1993)
10. Rawers, J., Govier, D., Cook, D.: bct-Fe formation during mechanical processing of bcc-Fe powder. *Scr. Metall. Mater.* **32**, 1319–1324 (1993)
11. Koyano, T., Chatani, K., Fukunaga, T., Mizutani, U.: Magnetic properties of Fe–V powders produced by mechanical alloying. *Mat. Science and Engineering* **A181/A182**, 1277–1280 (1994)
12. Rawers, J., Cook, D., Kim, T.: X-ray diffraction and Mössbauer characterization of attrition-milled nanostructured iron and iron–nitrogen powders. *Philos. Mag., A.* **78**, 965–977 (1998)
13. Le Caér, G., Ziller, T., Delcroix, P., Bellouard, C.: Mixing of iron with various metals by high-energy ball milling of elemental powder mixtures. *Hyperfine Interact.* **130**, 45–70 (2000)
14. Ziller, T., Le Caér, G., Isnard, O., Cenedese, P., Fultz, B.: Metastable and transient states of chemical ordering in Fe–V nanocrystalline alloys. *Phys. Rev. B* **65**, 024204 (2002) (14 p)
15. Kataoka, N., Sumiyama, K., Nakamura, Y.: Metastable crystalline and amorphous Fe–V alloys produced by vapor quenching. *Trans. Jpn. Inst. Met.* **27**, 823–829 (1986)
16. Ziller, T.: Étude du Mélange à l’État Solide lors de la Mécanosynthèse d’alliages Fe–X (X=Cr, Mn, V, Mo) et étude de la mise en ordre d’alliages Fe–V élaborés par cette technique. Ph.D. Thesis, Nancy (2000)
17. Williamson, G., Hall, W.H.: X-ray line broadening from filed aluminium and wolfram. *Acta Metall.* **1**, 22–31 (1952)
18. Le Caér, G., Dubois, J.M.: Evaluation of hyperfine parameter distributions from overlapped Mössbauer spectra of amorphous alloys. *J. Phys. E* **12**, 1083–1090 (1979)
19. Seki, J.I., Hagiwara, M., Suzuki, T.: Metastable order-disorder transition and sigma phase formation in Fe–V binary alloys. *J. Mater. Sci.* **14**, 2404–2410 (1979)
20. Le Caér, G., Brand, R.A.: General models for the distributions of electric field gradients in disordered solids. *J. Phys., Condens. Matter.* **10**, 10715–10774 (1998)
21. Shiga, M., Nakamura, Y.: Effect of local environment on formation of local moments in bcc Fe–V alloys: Mössbauer study. *J. Phys. F. Met. Phys.* **81**, 177–190 (1978)
22. Dubiel, S.M., Zinn, W.: Influence of V on the Fe site spin and charge densities in BCC-iron. *J. Magn. Magn. Mater.* **37**, 237–245 (1983)
23. Krause, J.C., Schaf, J., da Costa, M.I. Jr, Paduani, C.: Effect of composition and short-range order on the magnetic moments of Fe in $\text{Fe}_{1-x}\text{V}_x$ alloys. *Phys. Rev. B* **61**, 6196–6204 (2000)
24. Fu, C.L., Krčmar, M., Painter, G.S., Chen, X.Q.: Vacancy mechanism of high oxygen solubility and nucleation of stable oxygen-enriched clusters in Fe. *Phys. Rev. Lett.* **99**, 225502 (2007)